

Research Article

Multi-Band Antennas for 4G, 5G FR1 and Wi-Fi 6E/7 Bands in Smartwatch Devices

Yong-Zhi Su[✉], Wen-Shan Chen^{*✉}

Department of Electronic Engineering, Southern Taiwan University of Science and Technology, Tainan, Taiwan
E-mail: Chenws@stust.edu.tw

Received: 12 April 2024; **Revised:** 11 June 2024; **Accepted:** 21 June 2024

Abstract: This article introduces an antenna design for smartwatch applications, with an overall size is $45 \times 45 \times 5.4 \text{ mm}^3$. All antenna elements adopt the IFA (Inverted-F antennas) structures. The application bands include Global Positioning System (GPS), Wi-Fi 6E/7 with 2.4 GHz, 5.2 GHz, 5.8 GHz and 6 GHz bands, 4G LTE (Long Term Evolution) with B2 and B4, 5G n41, n77, n78, n79 bands, covering all Wi-Fi 6E/7 and the mainly bands of 5G FR1 bands. Additionally, this design also reserves a frequency band in the 6G mid-high band (6–9 GHz), ensures that design can be suitable for next generation of wireless systems. Furthermore, the antenna element designed for switching B2 and B4 bands to reduce the occupied space of the element. The design with five antennas and good performances can be applied to the bands of 4G, 5G FR1, and Wi-Fi 6E/7 systems in smartwatch applications.

Keywords: smartwatch antenna, Wi-Fi 6E/7, 5G FR1, 4G, switch, 6G

1. Introduction

After the rapid development of wireless communication, innovative applications for smart devices also emerged rapidly, such as Augmented Reality (AR), real-time health monitoring and high-quality video calls. Traditional smartwatches with limit computing capabilities and transmission speeds could only work in past world. In the past, the majority of wearable devices only supported older communication protocols like Long Term Evolution (LTE) or Wi-Fi 5, which could handle mild transmission requirements adequately. However, with increasing demands for transmission, smartwatch antennas need to be renewed to support higher transmission speeds and lower latency in the future.

Now, numerous references related to antennas on smart wearable devices have been proposed, and various structures are utilized in the design. For example, the coupled structure [1, 2] has a smaller size, which is advantageous for application in highly restricted space sizes. The Invert-F Antenna (IFA) structure [3, 4, 5, 6] has advantages such as superior matching and stability. The loop structure [7, 8] has wider modes, and it can be built on metal frame of smartwatches, according to size and shapes, ensuring maximize space utilization. The antenna design with coplanar waveguide (CPW) [9, 10] also features wider modes, achieving better matching and a smaller size simultaneously. Additionally, there is a different design that utilizes the watch strap and builds the antenna on it [11, 12], moving the antenna outside the smartwatch to a larger space, avoiding restrictions in space.

Along with various smart devices incorporating higher frequencies and wider application bands, such as Wi-Fi 6E/7 [13, 14, 15, 16] and 5G C-Bands [17, 18, 19, 20], there is a need to handle more stringent transmission requirements.

As transmission speed increases, new challenges arise, such as the increase in the number of antennas and frequencies, requiring more occupied space. However, current smartwatches designs have limited space, posing a significant challenge for designers. To address this issue, many antennas adopt a method of adding chip inductors and capacitors to the antenna elements. This method has various applications, including the addition of inductors to the paths [21, 22], reducing path length through the characteristics of inductors. Alternatively, more complicated methods, such as using impedance matching or other tuning ways [23, 24, 25, 26, 27], can alter current characteristics, significantly reducing the size of the antenna element.

This article offers a design of smartwatch antennas that can be applied in 4G/5G FR1 and Wi-Fi 6E/7. This antenna can support 5G FR1 application bands, including B2, B4, n41, n77, n78 and n79, covering the majority of 5G FR1 bands. This antenna also supported all bands of Wi-Fi 6E/7 systems, including 2.4 GHz, 5.2 GHz, 5.8 GHz and 6 GHz bands. This design adds an additional frequency band, GPS, commonly found in most mobile devices, this enables devices to support location services and provide navigation functions. A smartwatch antenna combines a simulated switch to change bands between at B4 and B2 in limited space, reducing the occupied space for mid-low frequency antennas. Because of the characteristics of IFA structure, chip inductors are added to reduce the antenna size, while it maintains the performance of antenna's gain and efficiency. This smartwatch offers variety of advantages, such as incorporating a simulated switch on the path, which helps reduce the occupied space. Furthermore, the antenna supports the majority of 5G Sub-6 bands and additionally support the 6G extended band (6–9 GHz), enabling the smartwatch antenna to transition to the next generation of wireless systems.

2. Antenna design and concepts

The structure of this smartwatch antenna is shown in Figures 1 and 2. The substrate used is 0.4 mm FR4 with a relative permittivity of 4.4. The overall size of the antenna is $45 \times 45 \times 5.4 \text{ mm}^3$, and the system ground is $35 \times 35 \text{ mm}^2$. It adopts 50-ohm feed for the current.

This antenna is built with five IFA structure antennas, and the details of antennas structure are shown in Figure 3. Figure 3a represents Ant. 1, which is used to resonate GPS band. This element included an inductor at the antenna's main path with an inductance of 5.6 nH. This design helps reducing the original resonate path length. Figure 3b represents Ant. 2, used to resonate LTE B2 and B4 bands, this antenna element adopts a simulated switch design, as shown in Figure 4a. The switch is placed on the main path of the antenna, and the inductance is 3.3 nH. Added an inductor on one side of switch helps change the main path's impedance matching, achieving the goal of using one path to resonate two frequencies. This antenna element can operate in two types, B4 type and B2 type, resonating B4 uplink band (1.71–1.755 GHz) and B2 bands (1.85–1.99 GHz) separately. The circuit diagrams are shown in Figure 4b,c. Figure 3d represents Ant. 4, used to resonate WLAN5, Wi-Fi 6E (6 GHz) and 6G extended application band. This antenna adopts a wide path to resonate main mode and combines with higher-order mode to achieve a wider bandwidth. Figure 3e represents Ant. 5, used to resonate 5G C-Bands, and there are n77, n78 and n79 separately. This antenna utilizes the main path and branch path to compose a dual-mode resonance. Additionally, this antenna element uses two inductors to change the antenna's resonant path length and impedance matching, and both inductances are 1 nH and 1.5 nH, respectively, which meets the requirements of matching and bandwidth. Dimensions of the antenna's elements are also listed in Table 1.

Figure 5 shows the current distribution chart, illustrating the resonating of the antenna elements. Figure 5a presents the chart for Ant. 1, resonating at 1.575 GHz. In this chart, it is evident that the application band of this antenna is resonates through the main path of IFA. Figure 5b–d shows the charts for Ant. 2 that resonating at 1.73, 1.92, and 2.13 GHz, respectively. In these charts, we can see that the 1.73 GHz resonance occurs through the main path, with the current flowing along the lower side of the simulated switch and through the chip inductor simultaneously. The 1.92 GHz resonance occurs through the upper side path of the switch, while the 2.13 GHz resonance occurs through branch path. Figure 5e presents the chart for Ant. 3, resonating at 2.53 GHz. This antenna also resonates through the main path of IFA. Figure 5f–h shows the charts for Ant. 5, resonating at 5.48, 6.52 and 8 GHz, respectively. Because the bands of this antenna create through both the main and higher modes, they exhibit similar current distribution performance in all three charts. The current is

distributed evenly on main path and some current flowing along the short path and reflowing to the ground plane. Lastly, Figure 5i-j shows resonance at 3.75 and 4.7 GHz, respectively, the lower bands resonance through the main path, while the higher band resonance through the branch path, demonstrating some coupled effects with main path simultaneously.

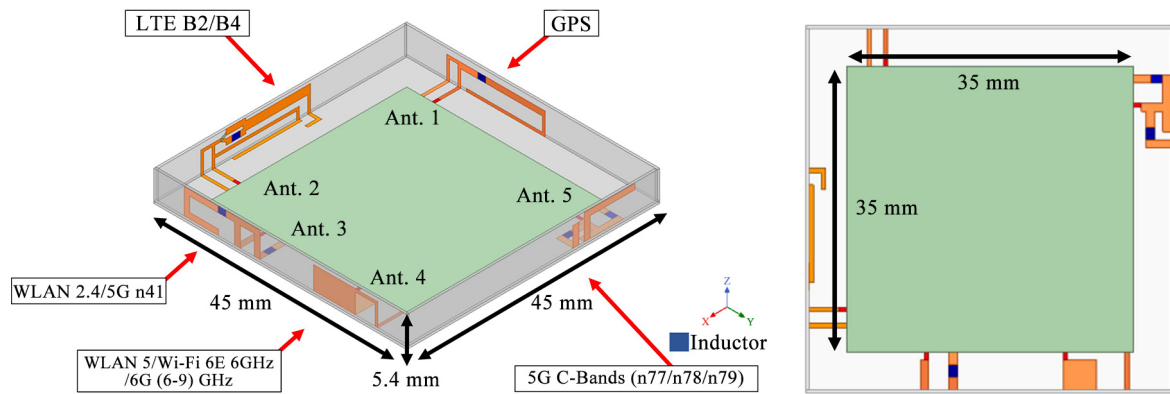
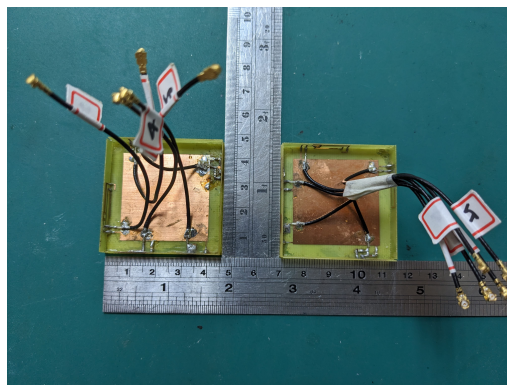
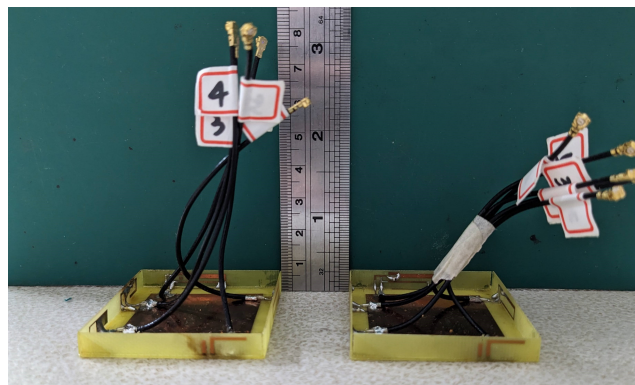


Figure 1. Simulated side view and overlook of smartwatch antenna



(a)



(b)

Figure 2. Measured of smartwatch antenna

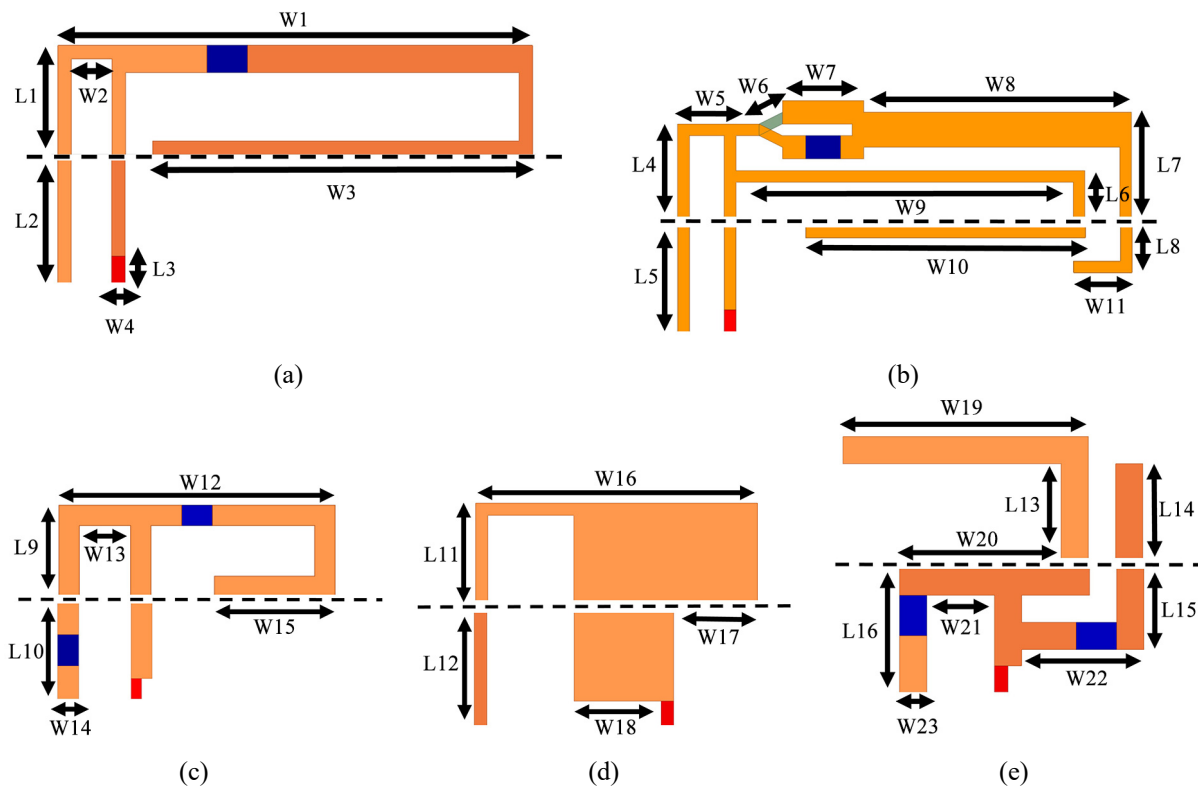


Figure 3. Details of antenna structure (a) Ant. 1, using to resonate GPS band, (b) Ant. 2, using to resonate B2 and B4 bands, (c) Ant. 3, using to resonate n41 and WLAN 2.4 bands, (d) Ant. 4, using to resonate WLAN 5, Wi-Fi 6E (6 GHz) and 6G mid-high extended bands, (e) Ant. 5, using to resonate 5G C-bands

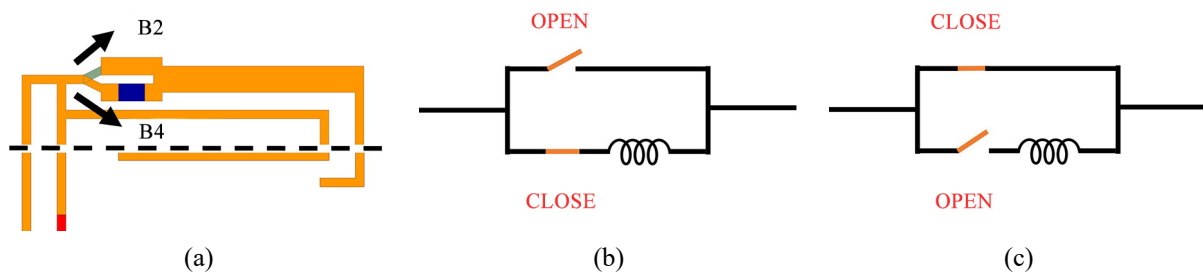


Figure 4. Ant. 2 with different switch types of antenna design and circuits diagrams (a) The antenna element place a switch on the main path, (b) B4 type (B4 Uplink band), (c) B2 type (B2 Bands)

Table 1. Detailed dimensions of the proposed antenna

Parameter	W1	W2	W3	W4	W5	W6	W7	W8
Unit (mm)	17.5	1.5	14	0.5	3.5	0.5	3.5	11.5
Parameter	W9	W10	W11	W12	W13	W14	W15	W16
Unit (mm)	14.5	12	2.5	13.5	2.5	1	6.1	11.5
Parameter	W17	W18	W19	W20	W21	W22	W23	
Unit (mm)	3.5	3.5	9	6	2.5	4.5	1	
Parameter	L1	L2	L3	L4	L5	L6	L7	L8
Unit (mm)	4	4.6	1	4	4.6	1	4.5	2
Parameter	L9	L10	L11	L12	L13	L14	L15	L16
Unit (mm)	4.5	4.6	4	4.6	3.5	3.5	3	4.6

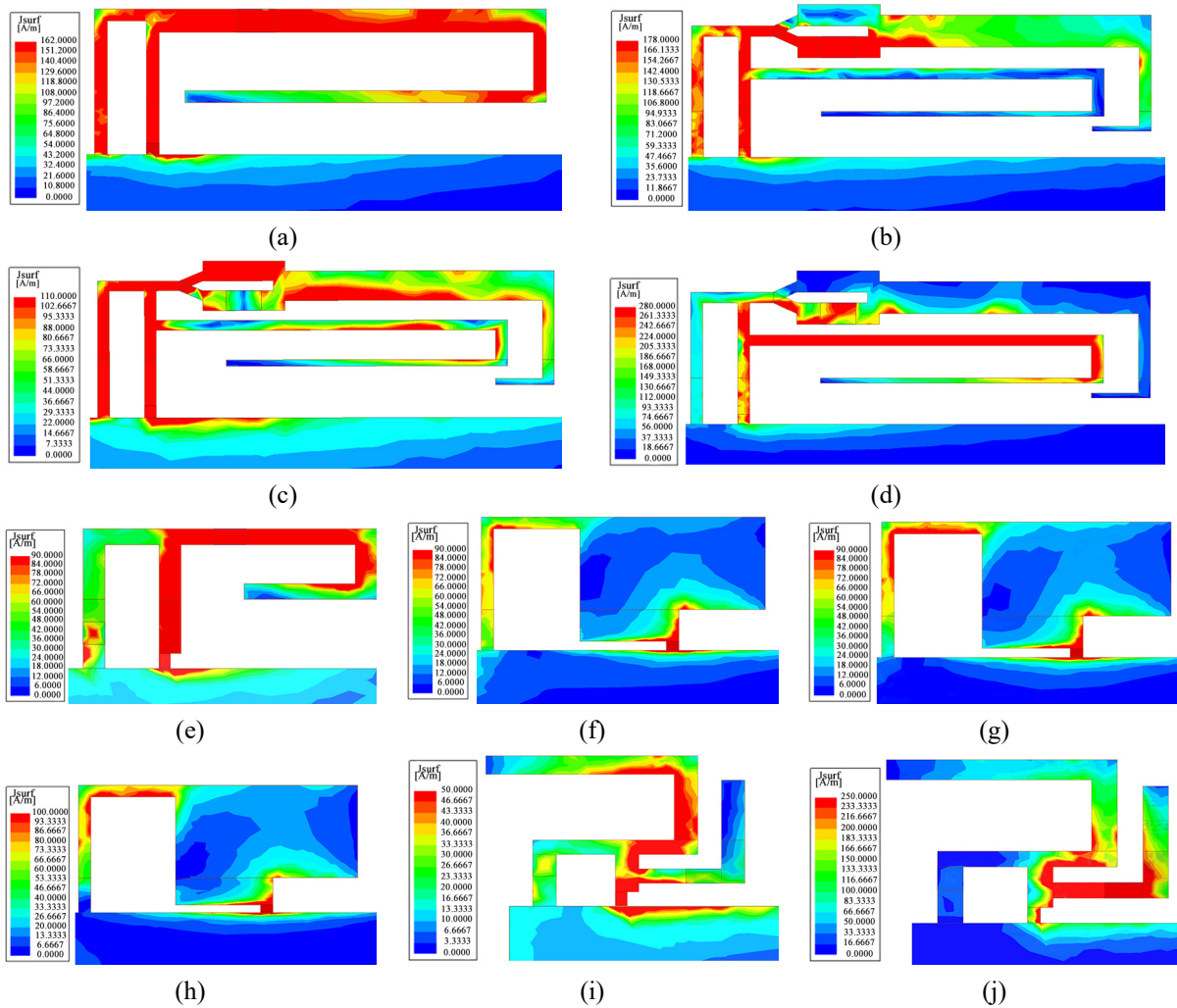


Figure 5. Simulated surface current distribution of antenna elements (a) resonating at 1.575 GHz (Port 1/B4 type), (b) resonating at 1.73 GHz (Port 2/B4 type), (c) resonating at 1.92 GHz (Port 2/B2 type), (d) resonating at 2.13 GHz (Port 2/B4 type), (e) resonating at 2.53 GHz (Port 3/B4 type), (f) resonating at 5.48 GHz (Port 4/B4 type), (g) resonating at 6.52 GHz (Port 4/B4 type), (h) resonating at 8 GHz (Port 4/B4 type), (i) resonating at 3.75 GHz (Port 5/B4 type), (j) resonating at 4.7 GHz (Port 5/B4 type)

3. Results and discussion

3.1 Parameters of proposed smartwatch antenna

This section will discuss the measured and simulated results of the proposed smartwatch antennas. All simulated results are created by using Ansys HFSS and CST Studio Suite. Figure 6 shows the 1–3 GHz S-parameters of the antenna for different types. All bands shown in Figure 6a include GPS, B4, Wi-Fi 2.4 GHz and n41 bands, and all bands are good impedance matching. The bands of antennas are defined as the S-parameter less than -6 dB for GPS and relative of 4G/5G bands, while Wi-Fi bands are defined as S-parameter less than -10 dB. Furthermore, Figure 6b shows the S-parameter of the other antennas, at the end of switch, in addition to the B4 uplink band changing to the B2 bands, the other bands maintain their respective matching. Figure 7 shows the 3–10 GHz S-Parameters of the antenna, separated into two types, including frequency bands in the range of 5G C-Bands (n77/n78/n79), WLAN5, Wi-Fi 6E/7 (6 GHz band) and 6G extended band. From Figure 7a,b, it can be observed that all of this antenna's bands have sufficient matching in both types. Combining the information from the above figures and values ensures that the matching is adequate after switching between both types.

Figure 8 shows the isolation S-parameters of the smartwatch antennas. In Figure 8a,b, they can be found the isolation parameter between the two types of antenna elements is less than -10 dB. Incorporating the S-parameters of the two type antennas ensures that the antenna elements can transmit data separately, and not disturbed by other antenna element in the smartwatch.

Figure 9 shows the step-wise design chart of antenna elements. This figure illustrates some important designs. Figure 9a shows the step-wise design of Ant. 2. Step 1 is the proposed design, which has a branch path, and step 2 decreases the branch path, This chart demonstrates the higher frequencies resonate through the branch path. Figure 9b shows the step-wise design of Ant. 4. This chart illustrates the resonating of the higher mode, decreasing the short path length helps control the higher mode, moving it to lower frequencies. Furthermore, duo to the decrease in short path length, it affects the matching of the main mode. It can be seen that the proposed design is the best situation compared to the others. Figure 9c shows the step-wise design of Ant. 3. Duo to this antenna consisting of dual modes, it needs to determine the resonating of antenna. Step 1 is the proposed design, which can be seen as built by main and branch path. In step 2, the higher mode vanishes duo to the decreased branch path, and in step 3, the inductor set in the short path is decreased. After this change, the antenna's matching is worse than in step 2. Figure 9 demonstrates the correct resonating and construction of the antenna elements, ensure that the characteristics of those are under control of the designer.

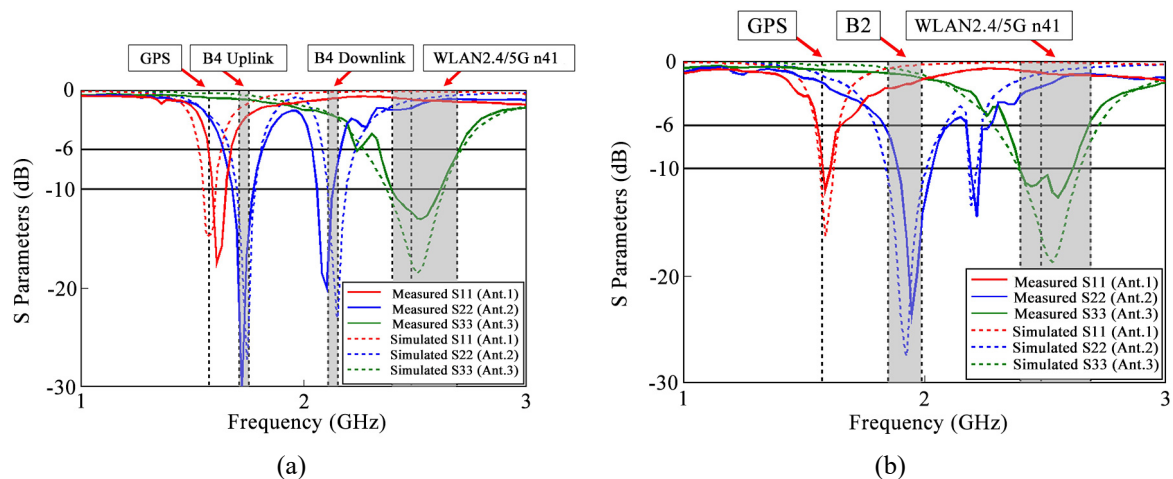


Figure 6. Antenna measured and simulated in 1–3 GHz S-Parameter (a) B4 type, (b) B2 type

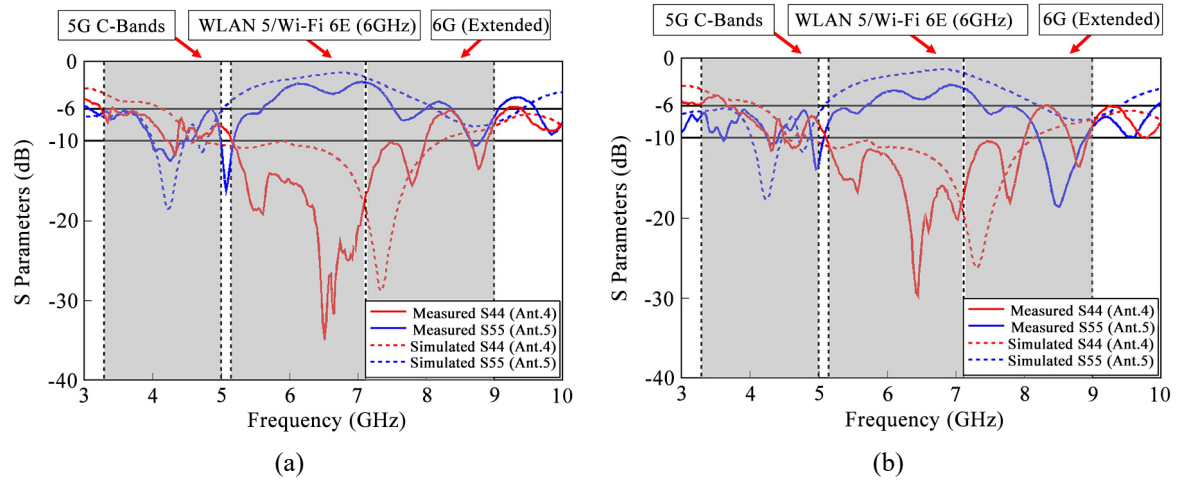


Figure 7. Antenna measured and simulated in 3–10 GHz S-Parameter (a) B4 type, (b) B2 type

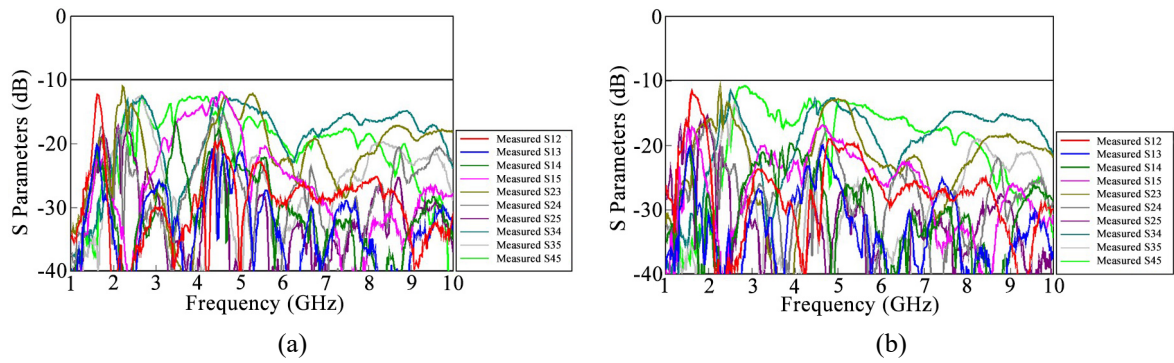


Figure 8. Antenna measured in 1–10 GHz isolation S-Parameters (a) B4 type, (b) B2 type

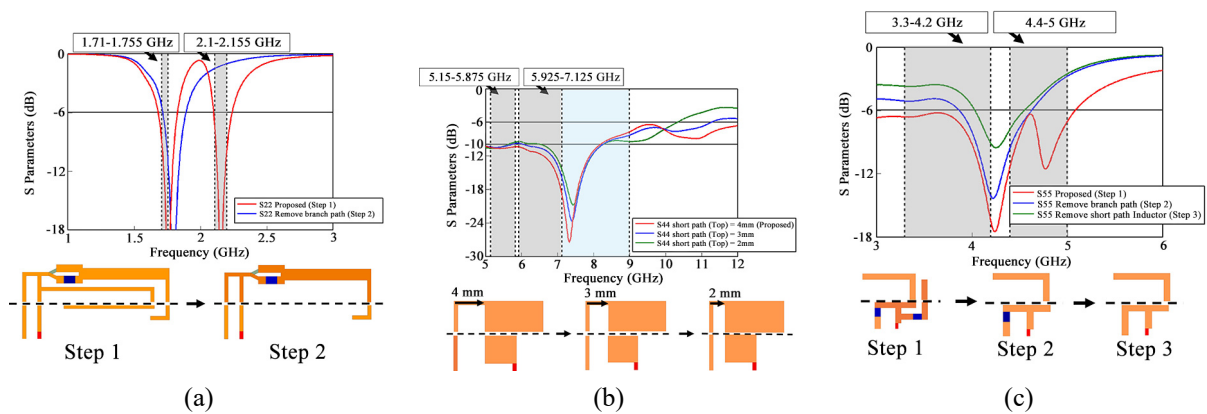


Figure 9. Step-wise design of antenna elements (a) Ant. 2 Step-wise chart (B4 type), (b) Ant. 4 Step-wise chart, (c) Ant. 5 Step-wise chart

3.2 Measured results of far field

Figure 10 shows the measured gain and efficiency of the smartwatch antennas. The all of far field testing are measured by chamber of ETS-Lindgren, the details of parameters and formula are in reference [28, 29]. In Figure 10a, the positioning of the antenna during testing is displayed, also included the measured far-field patterns. Duo to the antenna having two switch types, and both have same results, testing for B2 bands is conducted using the B2 type, while the results for other bands are obtained using the B4 type. Figure 10b shows the cases for Ant. 1 testing in the range of 1.56–1.595 GHz. The gain is ranging from -0.5 to 1 dBi; the efficiency is ranging from 45 to 64%. Figure 10c shows the cases for Ant. 2 testing in the range of 1.71–1.755 GHz. The gain is ranging from 2.2 to 2.7 dBi, and efficiency is ranging from 83–86%. Figure 10d shows cases for Ant. 2 testing in the range of 2.11–2.155 GHz. The gain is ranging from -1.1 to 1 dBi, and the efficiency is ranging from 31 to 47%. Figure 10e shows the cases for Ant. 2 testing in the range of 1.85–1.99 GHz. The gain is ranging from 1.9–3.2 dBi, and the efficiency is ranging from 68–87%. Figure 10f shows the cases for Ant. 3 testing in the range of 2.4–2.69 GHz. The gain is ranging from 0.2–2.4 dBi, and the efficiency is ranging from 35–69%. Figure 10g shows the cases for Ant. 4 testing in the range of 5.15–5.825 GHz. The gain is ranging from 2.2–4.9 dBi, and the efficiency is ranging from 57–84%. Figure 10h shows the cases for Ant. 4 testing in the range of 5.925–7.125 GHz. The gain is ranging from 2.8–4 dBi, and the efficiency is ranging from 54–80%. Figure 10i shows the cases for Ant. 4 testing in the range of 6–9 GHz. The gain is ranging from 2.6–3.3 dBi, and the efficiency is ranging from 51–72%. Figure 10j shows the cases for Ant. 5 testing in the range of 3.3–5 GHz. The gain is ranging from 0.5–3.1 dBi, and the efficiency is ranging from 23–36%.

Figure 11 presents the measured and simulated 2D radiation patterns of the design, Figure 11a shows the angle and scale chart of the 2D radiation patterns, with charts separated into the H plane (Magnetic Field Plane) and E plane (Electric Field Plane), represented in the XY, YZ and XZ planes. Furthermore, because this smartwatch antenna has a significant portion that is hand-made, there are some differences between the measure and simulated results. Figure 11b shows the radiation pattern of Ant. 1 tested at 1.575 GHz. In H plane, the radiation is directed in Y direction, and in the E2 plane, it's directed in Z direction, demonstrating that the antenna radiates in YZ direction with a nearly omnidirectional pattern. Figure 11c–e shows the radiation pattern of Ant. 2 tested at 1.73, 2.13 and 1.88 GHz, respectively. As these three bands resonate through the same antenna element, they have similar radiation results. In H plane, radiation is directed in X direction, and in E1 plane, it's directed in Z direction, indicating radiation in XZ direction with a pattern, which is similar to omnidirectional. Figure 11f shows the radiation pattern of Ant. 3 testing at 2.45 GHz. In H plane, radiation is directed in Y direction, and in E2 plane, it's directed in Z plane, indicating that the antenna radiating in YZ direction with a pattern, which is similar to omnidirectional. Figure 11g–j shows the radiation pattern of Ant. 4 tested at 5.26, 5.75 and 6.125 GHz, respectively. In H plane, the antenna doesn't have a specific radiation direction, while in E1 plane, radiation is directed in Z direction, indicating the antenna have radiation pattern similar with omnidirectional and not have specific directionality. Lastly, the radiation patterns of Ant. 5 tested in 3.4 and 4.6 GHz are shown. This antenna shows similar results to Ant. 4, that doesn't have accurate directionality and exhibiting an omnidirectional.

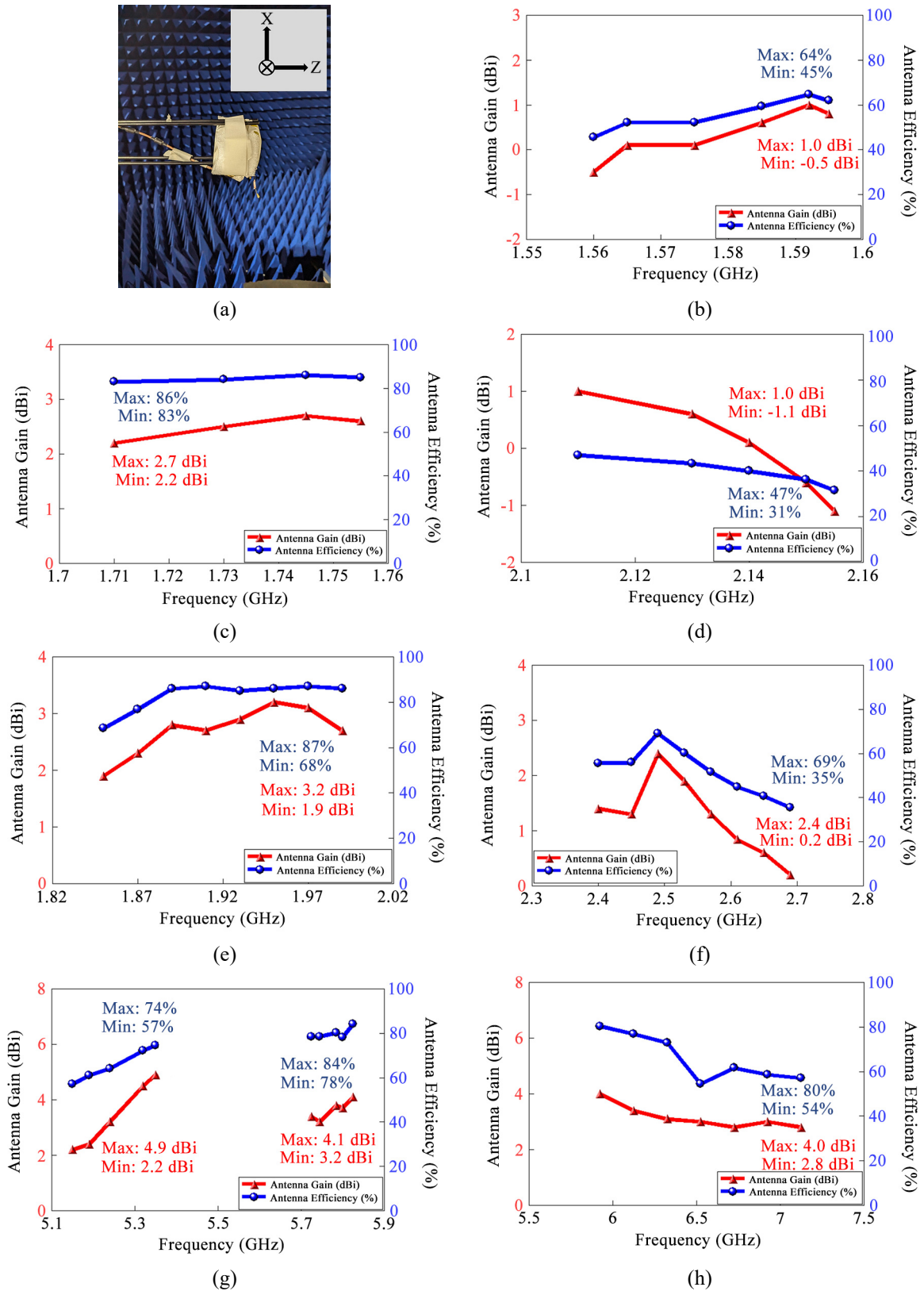


Figure 10. Cont.

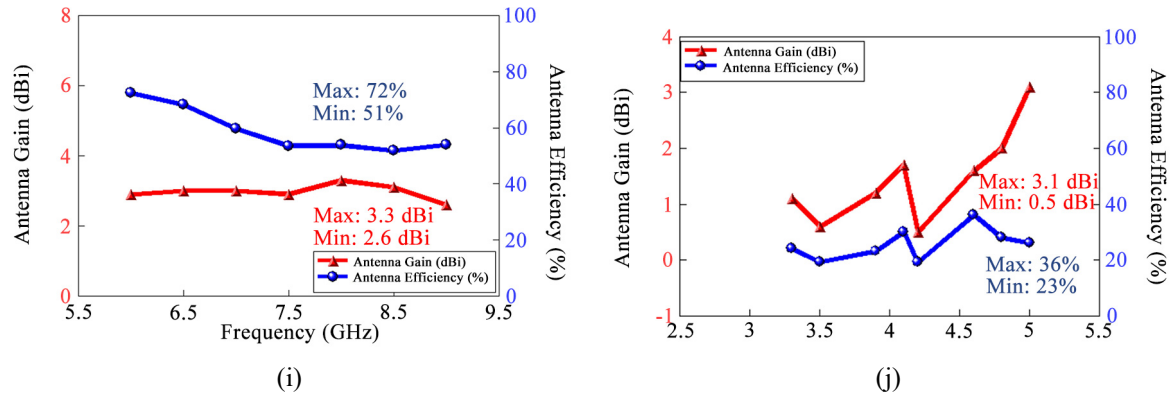


Figure 10. Measured gain and efficiency of antenna (a) The position of antenna in measuring, (b) Ant. 1 testing in 1.575–1.595 GHz (Resonating by Port 1/B4 type), (c) Ant. 2 testing in 1.71–1.755 GHz (Resonating by Port 2/B4 type), (d) Ant. 2 testing in 2.11–2.155 GHz (Resonating by Port 2/B4 type), (e) Ant. 2 testing in 1.85–1.99 GHz (Resonating by Port 2/B2 type), (f) Ant. 3 testing in 2.4–2.69 GHz (Resonating by Port 3/B4 type), (g) Ant. 4 testing in 5.15–5.825 GHz (Resonating by Port 4/B4 type), (h) Ant. 4 testing in 5.925–7.125 GHz (Resonating by Port 4/B4 type), (i) Ant. 4 testing in 6–9 GHz (Resonating by Port 4/B4 type), (j) Ant. 5 testing in 3.3–5 GHz (Resonating by Port 5/B4 type)

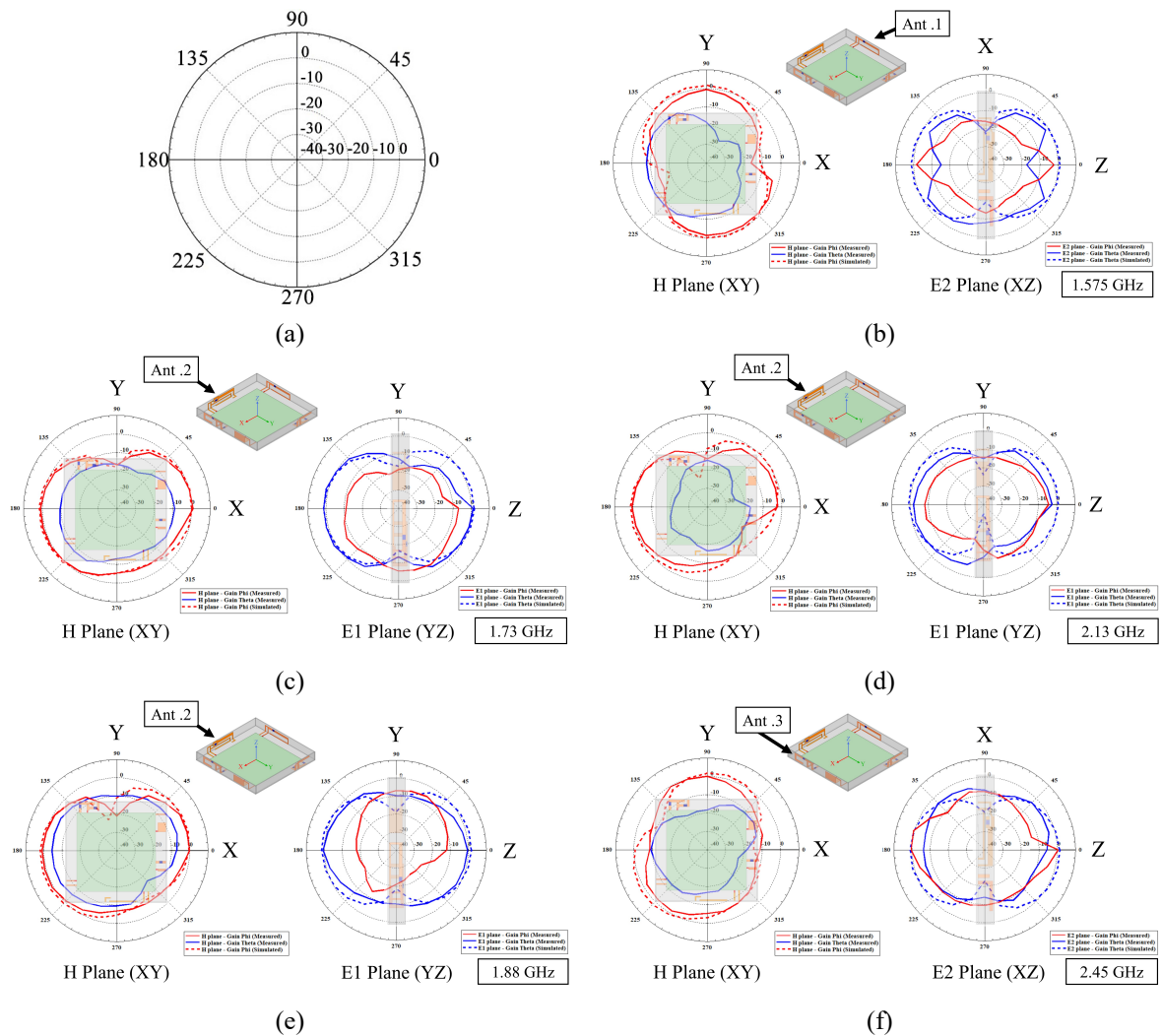


Figure 11. Cont.

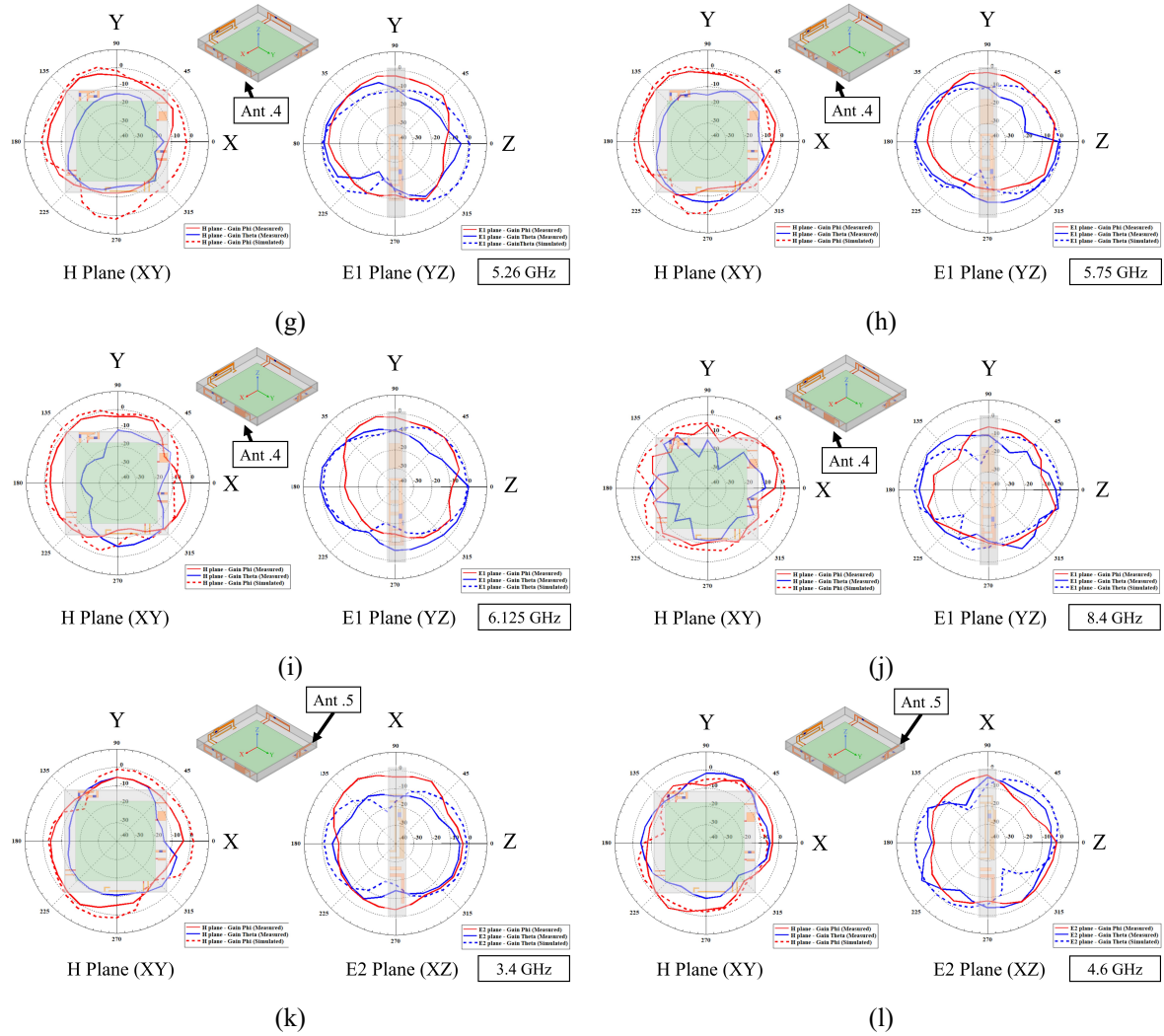


Figure 11. Measured and Simulated 2D Radiation patterns of antenna (a) Angle and Scale of 2D Radiation Fields, (b) Ant. 1 testing at 1.575 GHz (Resonating by Port 1/B4 type), (c) Ant. 2 testing at 1.73 GHz (Resonating by Port 2/B4 type), (d) Ant. 2 testing at 2.13 GHz (Resonating by Port 2/B4 type), (e) Ant. 2 testing at 1.88 GHz (Resonating by Port 2/B2 type), (f) Ant. 3 testing at 2.45 GHz (Resonating by Port 3/B4 type), (g) Ant. 4 testing at 5.26 GHz (Resonating by Port 4/B4 type), (h) Ant. 4 testing at 5.75 GHz (Resonating by Port 4/B4 type), (i) Ant. 4 testing at 6.125 GHz (Resonating by Port 4/B4 type), (j) Ant. 4 testing at 8.4 GHz (Resonating by Port 4/B4 type), (k) Ant. 5 testing at 3.4 GHz (Resonating by Port 5/B4 type), (l) Ant. 5 testing at 4.6 GHz (Resonating by Port 5/B4 type)

3.3 Simulated SAR results of smartwatch

Duo to the prolonged contact of smartwatches with human body, devices such as smartwatches, smartphones, and other wearables that transmit data wirelessly are required to be evaluated the Specific Absorption Rating (SAR) testing. After the test, these devices can be used in practical applications.

This simulated test was conducted in compliance with Federal Communications Commission (FCC) regulations governing wearable devices. According to FCC guidelines, the testing should be performed in units of 10 grams of tissue, with an average absorption rate not exceeding 4.00 W/kg. The simulated SAR results are shows in Figure 12 and were performed by using CST Studio Suite, with smartwatch and wrist positioned at a distance of 5 mm. Details of the SAR testing are provided in Table 2.

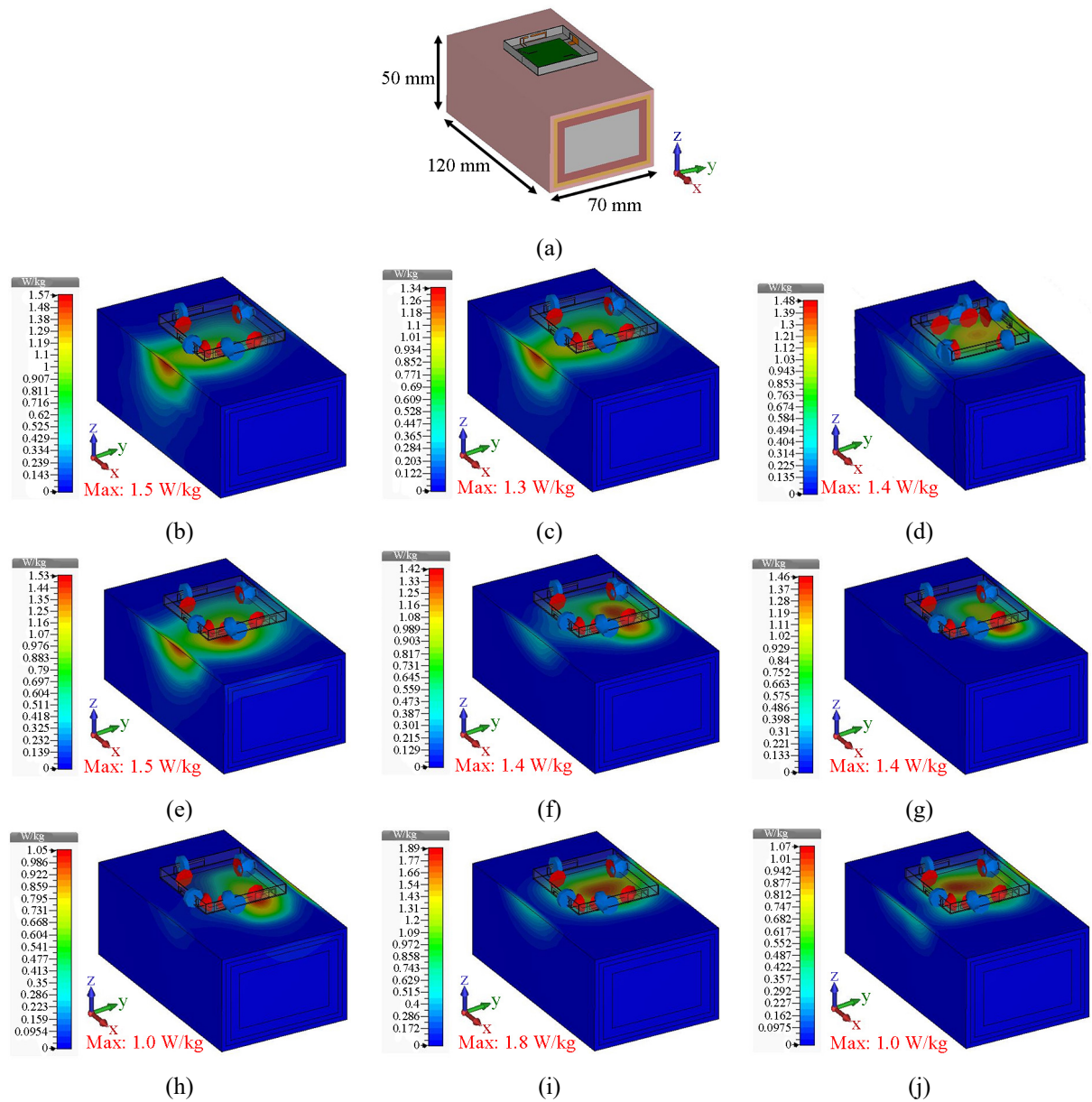


Figure 12. SAR simulation of smartwatch antennas with wrist (a) The position of antenna and wrist in simulation, (b) Ant. 2 test in 1.73 GHz, (c) Ant. 2 test in 2.13 GHz, (d) Ant. 2 test in 1.92 GHz, (e) Ant. 3 test in 2.54 GHz, (f) Ant. 4 test in 5.48 GHz, (g) Ant. 4 test in 6.525 GHz, (h) Ant. 4 test in 7.5 GHz, (i) Ant. 5 test in 3.75 GHz, (j) Ant. 5 test in 4.7 GHz

Table 2. Detailed SAR parameters for antenna worn on the wrist

10 g SAR (<4 W/kg)	Frequency	SAR (W/kg)
Ant. 2	2.49 GHz	2.2
Ant. 3	5.25 GHz	1.73
Ant. 3	5.775 GHz	1.76
Ant. 3	6.525 GHz	1.56
Ant. 4	5.25 GHz	1.76
Ant. 4	5.775 GHz	1.81
Ant. 4	6.525 GHz	1.55

3.4 Simulated radiation patterns of smartwatch with or without worn

This section will discuss the radiation fields of the antenna when worn or not on the wrist. Due to the prolonged contact of smartwatches with the body, the radiation direction or deflection may be changed as the result of body absorption. This test was simulated using CST Studio Suite, with a 5 mm gap between at the antenna and the wrist. The 2D radiation patterns for both types are listed in Table 3.

The simulated radiation patterns of the antenna without a wrist are similar to the measured patterns, and the radiation closely resembles omnidirectional distribution. Duo to the radiation with body absorption, after worn the smartwatch, the radiation of $-Z$ direction is reducing, and other way's radiation will change the direction close to $+Z$.

Table 3. Simulated radiation field difference between antenna with and without wrist wear

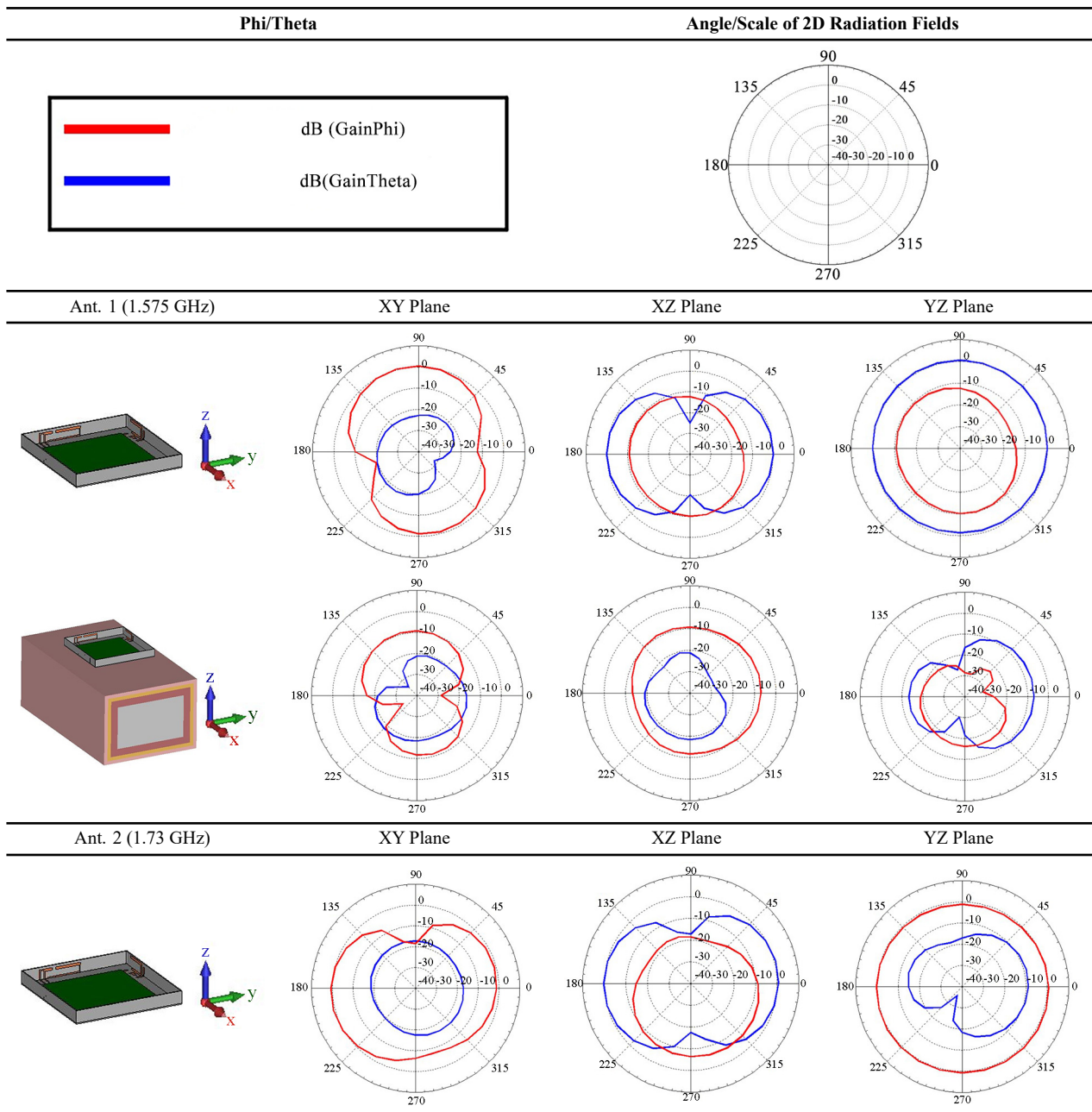


Table 3. Cont.

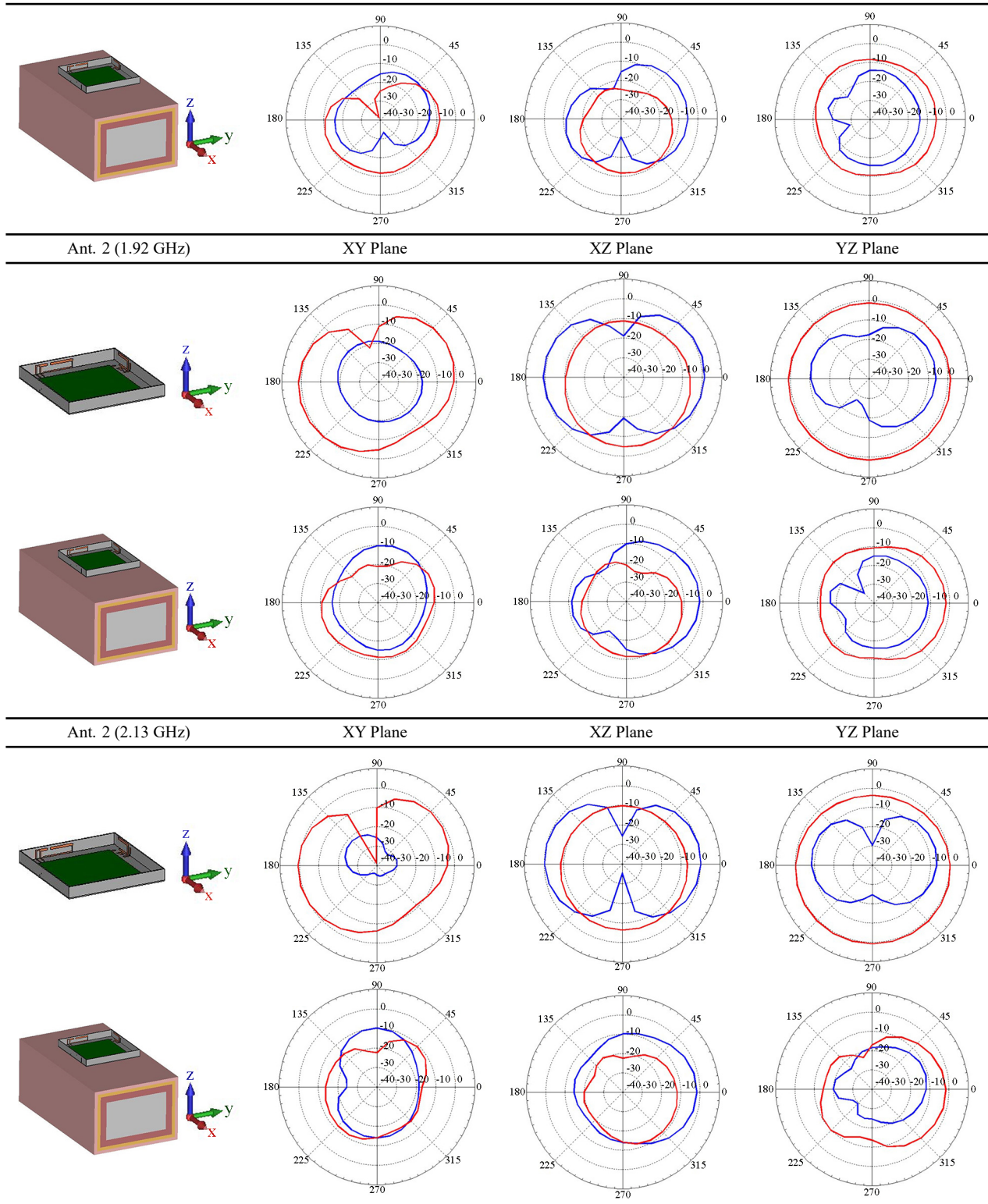


Table 3. Cont.

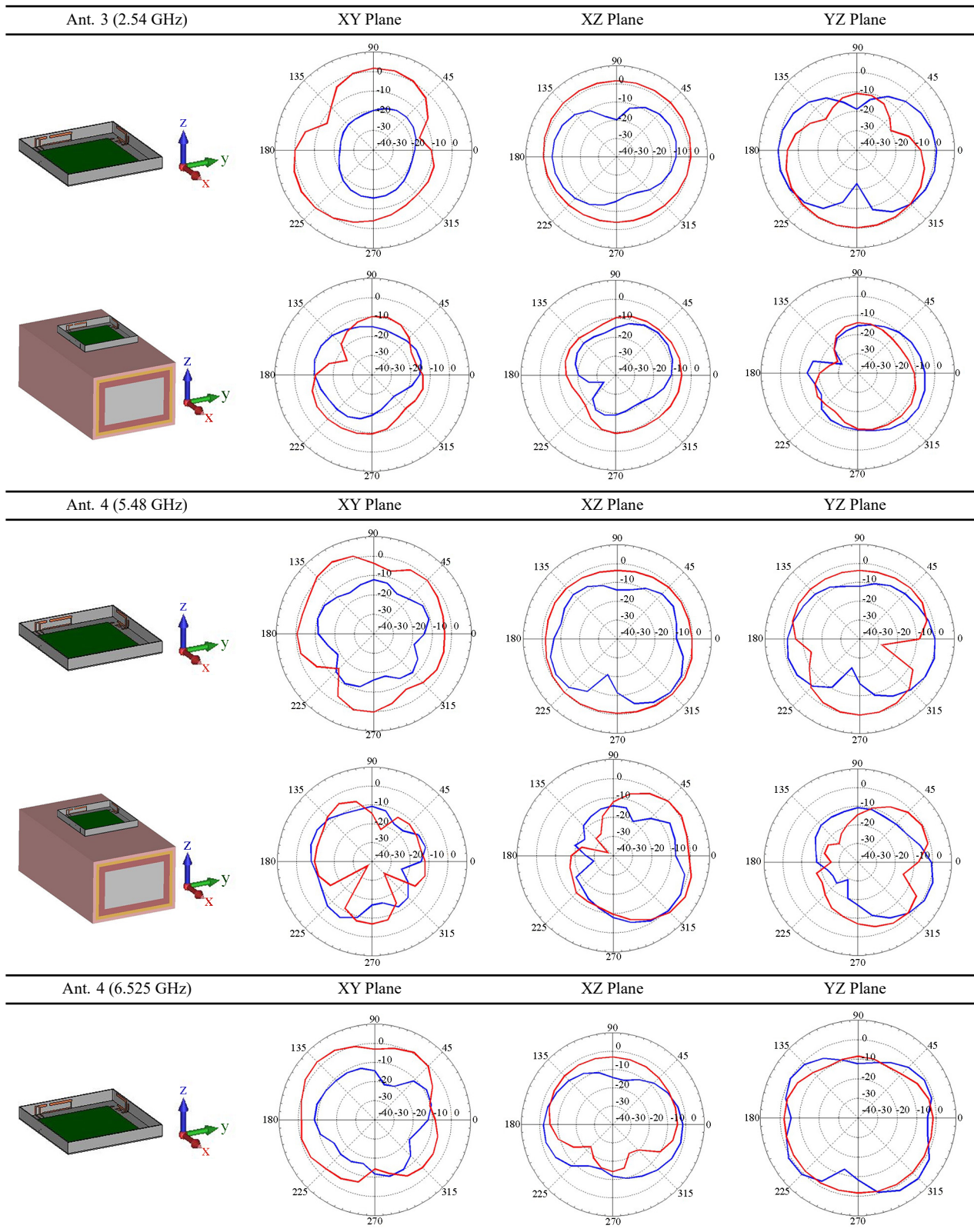


Table 3. Cont.

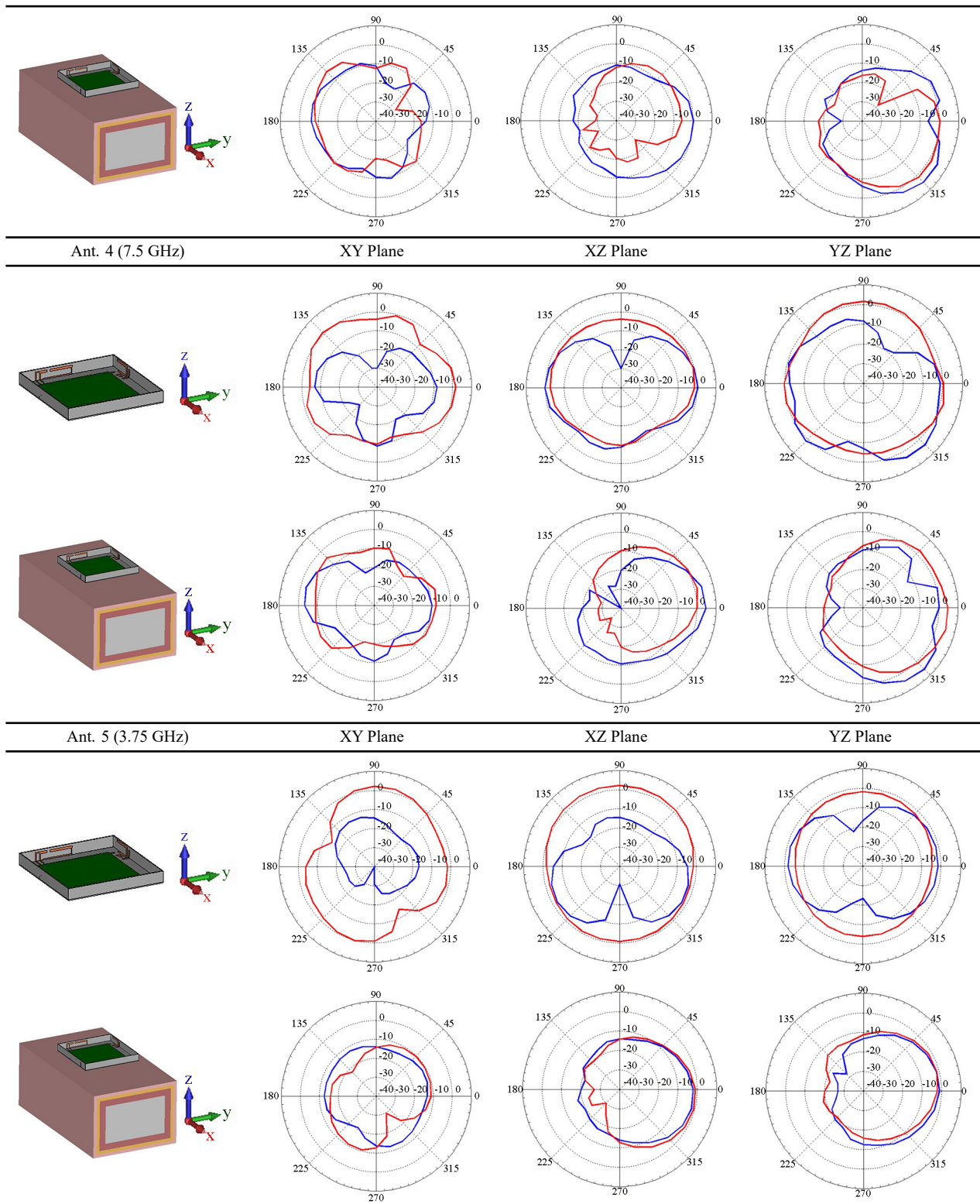
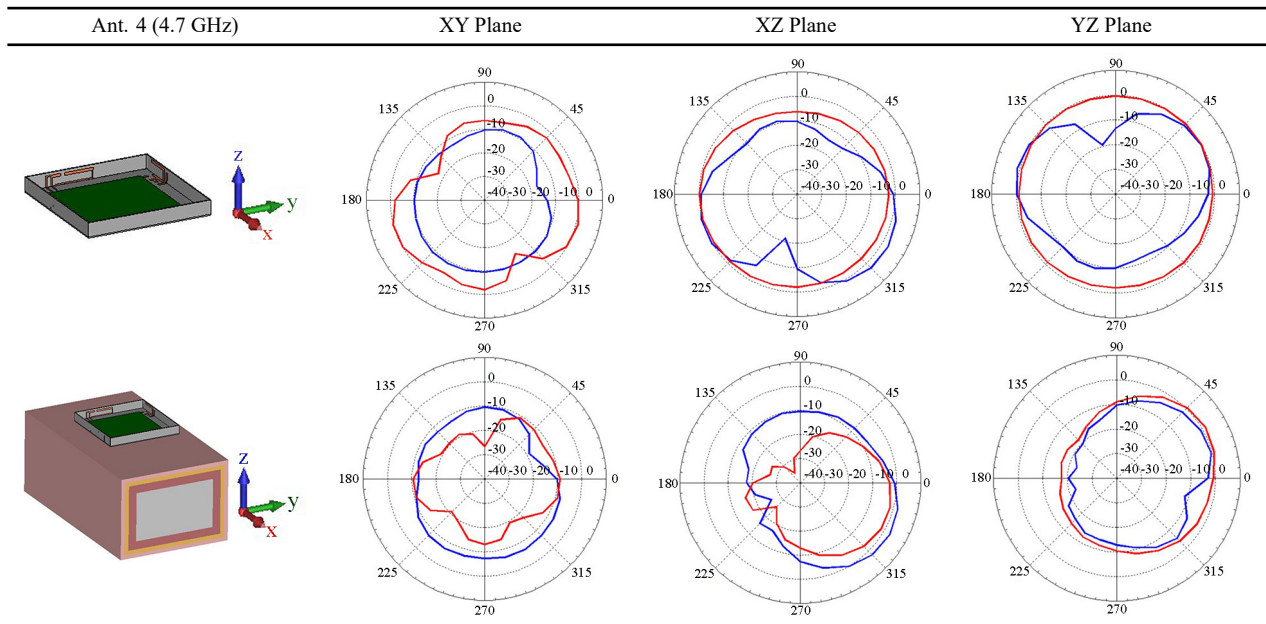


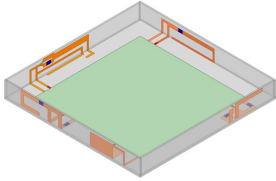
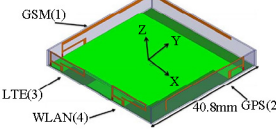
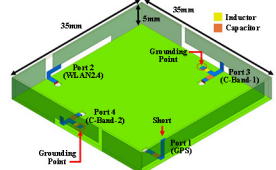
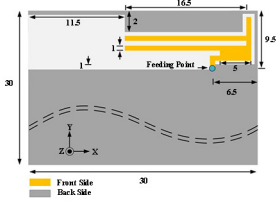
Table 3. Cont.



3.5 Comparison of smartwatch antennas with others

The Table 4 provides a comparison of the smartwatch antennas, including the antenna presented in this article and articles [1, 5, 30]. Since the proposed antenna and others have similar bands and applications, we can compare them accordingly. The antenna presented in reference [5] supports GSM, LTE, WLAN2.4 and GPS bands, with the goal of providing mobile communications. In reference [30], the antenna is designed for transmitting 5G communications, supporting WRC 5G bands, as well as WLAN 2.4 and GPS bands simultaneously. Lastly, reference [1] describes a smaller antenna capable of supporting LTE bands, while also enhancing support for Wi-Fi and location bands. This enables the antenna to operate flexibly across various applications. Compared to the four antennas, the proposed antenna stands out with a significant advantage in supporting a majority of 5G FR1 and Wi-Fi 6E/7 bands, enabling the smartwatch to operate in low, mid, and higher bands. While the proposed antenna currently doesn't include antenna elements for the 700–900 MHz bands due to the size constraints, it is compatible with most 5G FR1 bands. Additionally, other antennas may offer distinct advantages, such as more beauty, compactness and simplicity. Through the table can know about the advantages of these antennas, allowing users to choose based on their requirements or preferences. Furthermore, this chart also compares the average gain and efficiency of smartwatch antennas. In reference [5], gain and efficiency are 0.7 dBi and 46.2% separately. In reference [30], gain and efficiency are 0.5 dBi and 46.2% separately. In reference [1], gain and efficiency are 0.1 dBi and 85.2% separately. Lastly, the proposed antenna in this article has an average gain and efficiency of 2 dBi and 59.6%. Reference [1] shows best efficiency performance in the table, but the far field results of the antenna are simulated, which differs from measured results. In conclusion, the antennas of the design compared in this table have an efficiency performance higher than 40%, indicating good transmission performance for each antenna.

Table 4. Comparison chart of smart watch antennas

Antenna	Overall Size	Gain and Eff. (Average)	Structure	Application Bands	Year/Ref.
	$45 \times 45 \times 5.4 \text{ mm}^3$	Gain: 2.0 dBi Eff.: 59.6 % (Measured)	IFA	GPS LTE B2/B4 5G n41/C-Bands Wi-Fi 6E Bands	2024 (Proposed)
	$40.8 \times 40.8 \times 5.4 \text{ mm}^3$	Gain: 0.74 dBi Eff.: 46.2 % (Measured)	IFA	GSM 900 GPS LTE 2300 WLAN 2.4	2017 [5]
	$35 \times 35 \times 5 \text{ mm}^3$	Gain: 0.5 dBi Eff.: 46.2 % (Measured)	Open Slot	GPS WLAN 2.4 WRC 5G C-Band	2019 [30]
	$30 \times 30 \times 0.5 \text{ mm}^3$	Gain: 0.1 dBi Eff.: 85.2 % (Simulated)	Coupled	Galileo/GPS/Glonass GSM 1800/1900 UMTS/LTE 2300/2500 WLAN 2.4/5 WiMAX	2018 [1]

4. Conclusions

Duo to the rapid development of smart devices, applications of wearable devices are also increasing. The transmission requirements for wearable devices are more stringent. This article introduces a design of smartwatch antennas for 4G, 5G, and Wi-Fi 6E/7. The application frequency bands include GPS, all Wi-Fi 6E/7 bands, LTE B2 and B4 and 5G C-Bands. Additionally, the design reserves a mid-high band (6–9 GHz) for 6G extended band ensuring compatibility with future generation of wireless systems. In terms of design the antenna utilizes inductors and a simulated switch to reduce its size, and it adopts space diversity to address isolation issues between antenna elements, enabling simultaneous and separate transmission and reception of signals. Furthermore, the antenna undergoes various testing, including simulated SAR, measured gain and efficiency. Finally, the article examines the simulated radiation field with and without wrist wear, ensuring reliable signal transmission and reception in different scenarios.

Conflict of interest

The authors declare no conflict of interest.

References

- [1] S. Ahmad, M. Shahzad, and A. A. Alam, "A Compact Size ISM Band Wearable Flexible Antenna for IoT Smart Watch Applications," in *Proc. 1st Int. Conf. Microw., Antennas Circuits (ICMAC)*, Islamabad, Pakistan, Dec. 21–22, 2021. <https://doi.org/10.1109/ICMAC54080.2021.9678256>.
- [2] A. J. Khalilabadi and A. Zadehgo, "An Ultra-thin Dual-Band Smart-watch Antenna Compatible with Several Wireless Bands," in *Proc. IEEE Int. Symp. Antennas Propag. & USNC/URSI Nat. Radio Sci. Meeting*, Boston, MA, USA, Jul. 8–13, 2018. <https://doi.org/10.1109/APUSNCURSINRSM.2018.8608488>.
- [3] H. S. Huang, H. L. Su, and S. L. Chen, "Multiband antennas for GPS/GSM1800/Bluetooth/Wi-Fi smart watch applications," in *Proc. IEEE Int. Conf. Comput. Electromagn. (ICCEM)*, Kumamoto, Japan, Mar. 8–10, 2017. <https://doi.org/10.1109/COMPEN.2017.7912745>.
- [4] B. A. Baloch, Z. Zahid, and A. A. Khan, "Self-Decoupled Dual Band PIFA for Wi-Fi 6E Smartwatch MIMO Applications," in *Proc. 19th Int. Bhurban Conf. Appl. Sci. Technol. (IBCAST)*, Islamabad, Pakistan, Aug. 16–20, 2022. <https://doi.org/10.1109/IBCAST54850.2022.9990453>.
- [5] W. S. Chen, G. Q. Lin, and W. H. Hsu, "WLAN MIMO antennas with a GPS antenna for smart watch applications," in *Proc. Int. Workshop Electromagn., Appl. Student Innov. Compet.*, London, UK, May 30, 2017. <https://doi.org/10.1109/iWEM.2017.7968771>.
- [6] W. S. Chen, G. Q. Lin, and C. Y. D. Sim, "Multiband antennas for GSM/GPS/LTE/WLAN smart watch applications," in *Proc. 6th Asia-Pac. Conf. Antennas Propag. (APCAP)*, Xi'an, China, Oct. 16–19, 2017. <https://doi.org/10.1109/APCAP.2017.8420476>.
- [7] J. Li, Z. Wang, J. Wang, M. Leach, R. Pei, E. G. Lim, and Y. Luo, "Integrated Loop Antenna for Smartwatch," in *Proc. IEEE Int. Symp. Antennas Propag. & USNC-URSI Radio Sci. Meeting (APS/URSI)*, Singapore, Singapore, Dec. 4–10, 2021. <https://doi.org/10.1109/APS/URSI47566.2021.9704469>.
- [8] T. Y. Zhuo, W. S. Chen, and C. Y. D. Sim, "WLAN MIMO antennas for smart watch applications," in *Proc. IEEE Int. Symp. Electromagn. Compat. & Asia-Pac. Symp. Electromagn. Compat. (EMC/APEMC)*, Suntec City, Singapore, May 14–18, 2018. <https://doi.org/10.1109/ISEMC.2018.8394094>.
- [9] J. Kulkarni, B. Garner, and Y. Li, "A 3D-Printed Wide-Band Wrist-Worn Wearable Antenna for 4G/5G Wireless Communication," in *Proc. IEEE Int. Symp. Antennas Propag. & USNC-URSI Radio Sci. Meeting (USNC-URSI)*, Portland, OR, USA, Jul. 23–28, 2023. <https://doi.org/10.1109/USNC-URSI52151.2023.10237960>.
- [10] J. Kulkarni and C. Y. D. Sim, "Wideband CPW-Fed Oval-Shaped Monopole Antenna for Wi-Fi5 and Wi-Fi6 Applications," *PIERC*, vol. 107, pp. 173–182, 2021. <https://doi.org/10.2528/PIERC20110903>.
- [11] K. Zhao, Z. Ying, and S. He, "Antenna designs of smart watch for cellular communications by using metal belt," in *Proc. 9th Eur. Conf. Antennas Propag. (EuCAP)*, Lisbon, Portugal, Apr. 13–17, 2015.
- [12] K. Abdelhakim, M. Cabedo-Fabrés, and M. F. Bataller, "PIFA antenna for smart watch application in the 2.4 GHz band," in *Proc. IEEE Int. Symp. Antennas Propag. & USNC-URSI Radio Sci. Meeting (APS/URSI)*, Singapore, Singapore, Dec. 4–10, 2021. <https://doi.org/10.1109/APS/URSI47566.2021.9704480>.
- [13] S. W. Su, D. P. Yusuf, and F. H. Chu, "Conjoined, Wi-Fi 6E MIMO Antennas for Laptops," in *Proc. Int. Symp. Antennas Propag. (ISAP)*, Taipei, Taiwan, Oct. 19–22, 2021. <https://doi.org/10.23919/ISAP47258.2021.9614384>.
- [14] M. I. Magray and S. W. Su, "Conformal and Highly Compact Wi-Fi 6E Antenna for Laptop Applications," in *Proc. Asia-Pac. Microw. Conf. (APMC)*, Yokohama, Japan, Nov. 29, 2022. <https://doi.org/10.23919/APMC55665.2022.9999900>.
- [15] C. Y. D. Sim, J. Kulkarni, A. M. Apte, C. C. Cao, C. C. Chen, S. H. Wang, Y. U. Shu, and H. Z. Lai, "A PIFA Design with WLAN and Wi-Fi 6E Band for Laptop Computer Applications," in *Proc. IEEE Int. Symp. Antennas Propag. & USNC-URSI Radio Sci. Meeting (AP-S/URSI)*, Denver, CO, USA, Jul. 10–15, 2022. <https://doi.org/10.1109/AP-S/USNC-URSI47032.2022.9886623>.
- [16] C. Y. D. Sim, V. Dhasarathan, T. K. Tran, J. Kulkarni, B. A. Garner, and Y. Li, "Mutual Coupling Reduction in Dual-Band MIMO Antenna Using Parasitic Dollar-Shaped Structure for Modern Wireless Communication," *IEEE Access*, vol. 11, pp. 5617–5628, 2023. <https://doi.org/10.1109/ACCESS.2023.3235761>.
- [17] X. T. Yuan, Z. Chen, T. Gu, and T. Yuan, "A Wideband PIFA-Pair-Based MIMO Antenna for 5G Smartphones," *IEEE Antennas Wireless Propag. Lett.*, vol. 20, pp. 371–375, 2021. <https://doi.org/10.1109/LAWP.2021.3050337>.

- [18] W. Hu, Q. Li, H. Wu, Z. Chen, L. Wen, W. Jiang, and S. Gao, "Dual-Band Antenna Pair With High Isolation Using Multiple Orthogonal Modes for 5G Smartphones," *IEEE Trans. Antennas Propag.*, vol. 71, pp. 1949–1954, 2023. <https://doi.org/10.1109/TAP.2022.3233458>.
- [19] C. Y. D. Sim, H. D. Chen, J. Kulkarni, J. J. Lo, and Y. C. Hsuan, "Recent Designs to Achieving Wideband MIMO Antenna for 5G NR Sub-6GHz Smartphone Applications," in *Proc. Int. Symp. Antennas Propag. (ISAP)*, Osaka, Japan, Jan. 25–28, 2021. <https://doi.org/10.23919/ISAP47053.2021.9391444>.
- [20] C. Y. D. Sim, H. Y. Liu, and C. J. Huang, "Wideband MIMO Antenna Array Design for Future Mobile Devices Operating in the 5G NR Frequency Bands n77/n78/n79 and LTE Band 46," *IEEE Antennas Wireless Propag. Lett.*, vol. 19, pp. 74–78, 2020. <https://doi.org/10.1109/LAWP.2019.2953334>.
- [21] S. Lokesh, S. Karthick, C. Babu, and S. Gowtham, "Analyse and Design a micro strip spiral monopole antenna with and without indicator," in *Proc. 3rd Int. Conf. Comput. Methodol. Commun. (ICCMC)*, Erode, India, Mar. 27–29, 2019. <https://doi.org/10.1109/ICCMC.2019.8819769>.
- [22] Q. Luo, H. M. Salgado, and J. R. Pereira, "Compact printed C-shaped monopole antenna with chip inductor," in *Proc. IEEE Int. Symp. Antennas Propag. (APSURSI)*, Spokane, WA, USA, Jul. 3–8, 2011. <https://doi.org/10.1109/APS.2011.5996665>.
- [23] M. Ye, Y. Zhang, C. Wu, J. Cheng, and Z. Liu, "Dual-band Inverted-F Antenna with Tunable Inductor and Capacitor for 5G Mobile Communication," in *Proc. IEEE Int. Conf. Integr. Circuits, Technol. Appl. (ICTA)*, Beijing, China, Nov. 21–23, 2018. <https://doi.org/10.1109/CICTA.2018.8706075>.
- [24] K. L. Wong and C. Y. Tsai, "IFA-Based Metal-Frame Antenna Without Ground Clearance for the LTE/WWAN Operation in the Metal-Casing Tablet Computer," *IEEE Trans. Antennas Propag.*, vol. 64, pp. 53–60, 2016. <https://doi.org/10.1109/TAP.2015.2503420>.
- [25] W. C. Wu and K. L. Wong, "Metal-frame inverted-F antenna for the LTE metal-casing smartphone," in *Proc. Int. Symp. Antennas Propag. (ISAP)*, Okinawa, Japan, Oct. 24–28, 2016.
- [26] P. Y. Qin, F. Wei, and Y. J. Guo, "A Wideband-to-Narrowband Tunable Antenna Using A Reconfigurable Filter," *IEEE Trans. Antennas Propag.*, vol. 63, pp. 2282–2285, 2015. <https://doi.org/10.1109/TAP.2015.2402295>.
- [27] S. L. Chen, P. L. Qin, Y. J. Guo, and X. Chen, "A Multi-linear Polarization Reconfigurable Unidirectional Patch Antenna," *IEEE Trans. Antennas Propag.*, vol. 65, pp. 4299–4304, 2017. <https://doi.org/10.1109/TAP.2017.2712185>.
- [28] J. Kulkarni, N. Kulkarni, and A. Desai, "Development of "H-Shaped" monopole antenna for IEEE 802.11a and HIPERLAN 2 applications in the laptop computer," *Int. J. RF Microw. Comput. Aided Eng.*, vol. 30, 2020. <https://doi.org/10.1002/mmce.22233>.
- [29] "Antenna Pattern Measurement: Concepts and Techniques," ETS-Lindgren, Accessed: Jun. 21, 2024. [Online]. Available: <https://www.ets-lindgren.com/WhitePapers/APM.pdf>.
- [30] W. Z. Lee and W. S. Chen, "An antenna design on metal frame of smart watch," in *Proc. Int. Workshop Electromagn., Appl. Student Innov. Compet. (iWEM)*, Qingdao, China, Sep. 18–20, 2019. <https://doi.org/10.1109/iWEM.2019.8887882>.